JOURNAL OF APPLIED ELECTROCHEMISTRY **24** (1994) 894–899

Anodic film on lead–arsenic alloy in sulphuric acid medium

S.-J. XIA, W.-F. ZHOU*

Department of Chemistry, Fudan University, Shanghai, 200433, China

Received 22 October 1993; revised 14 January 1994

The phase composition, anodic behaviour and semiconducting properties of the anodic film on Pb–6 at % As alloy have been investigated. The linear relationship between i and $t^{-1/2}$ shows that the anodic film growth is controlled by a diffusion mechanism. The experimental results show that the anodic film contains t–PbO, $PbO \cdot PbSO_4$, $3PbO \cdot PbSO_4$ and some arsenic compounds. The dielectric constant of the film is 2.8×10^2 obtained from the capacitance–time relationship measured at 2500 Hz. The Mott–Schottky plot shows that the film is an n-type semiconductor. The flat-band potential is −0.56 V vs Hg/Hg_2SO_4, and the donor density is $7.2 \times 10^{15}\,cm^{-3}$ for the film obtained at 0.9 V vs Hg/Hg_2SO_4 for 2 h on a Pb–6 at % As electrode.

1. Introduction

The grid of the positive plate in a lead acid battery is usually made of lead alloy. Most of the lead alloys contain antimony, arsenic, tin, or other alloying additives. Owing to the anodic oxidation of the alloys, these additives become incorporated in both the corrosion layer and the active mass. It has been proved that such elements exert a considerable effect on the performance of the plate [1].

The effect of arsenic on the properties of lead acid battery positive plates has been reported to some extent [1–3]. Generally, the previous work concentrates on the capacity, the structure of the active mass and the cycle number. But the effect of arsenic on the lead anodic film has been little studied. The present study of the phase composition, anodic behaviour and semiconducting properties of the anodic film is aimed at better understanding of the effect of arsenic on the corrosion behaviour of the positive plate.

2. Experimental details

The electrolytic cell and electrode treatment have been described previously [4]. All the potentials mentioned in this paper are relative to that of a Hg/Hg_2SO_4 reference electrode containing the same solution as that in the electrochemical cell. The 4.5 M H_2SO_4 electrolyte was prepared from AR grade H_2SO_4 and triply distilled water at 25° C. It was used for both the cell and the reference Hg/Hg_2SO_4 electrode. The cell was maintained at $25 \pm 0.1°$ C.

Chronoamperometry and cyclic voltammetry were carried out using a PARC 273 Potentiostat/Galvanostat in conjunction with an X–Y recorder. A.c. impedance measurements were conducted with a PARC 378 a.c. impedance system. The working frequency range was selected as $10^3\,Hz < f < 10^4\,Hz$ (*vide infra*). All impedance measurements were made by applying to the working electrode a small signal amplitude of 5 mV(r.m.s.).

The analysis of the phase composition and depth profile of the anodic film were performed with a Rigaku D/max–γ B X-ray diffractometer and a Perkin–Elmer PHI 550 ESCA/SAM, respectively.

3. Results and discussion

3.1. *XRD analysis*

Table 1 presents the X-ray diffraction pattern of the anodic film obtained on a Pb–6 at % As electrode in 4.5 M H_2SO_4 at 0.9 V for 5 h.

It is observed that the anodic film contains $PbSO_4$, t-PbO, $PbO \cdot PbSO_4$, and $3PbO \cdot PbSO_4$. It has been proved that the phase composition of the anodic film on pure lead is t-PbO, o-PbO, $PbSO_4$ and $PbO \cdot PbSO_4$ [5]. The existence of arsenic changes the phase composition formed by the anodic oxidation in lead–arsenic alloys.

No diffraction lines of As_2O_3 are given in Table 1.

3.2. *Auger depth profile of the anodic film*

Figure 1 shows the Auger depth profile of the anodic film obtained at 0.9 V on a Pb–6 at % As electrode for 2 h.

The anodic film contains Pb, O, As and S elements. Among all the elements the atomic percentage of lead in the film is the highest, and the atomic percentage of oxygen is less than that of lead. This indicates some unoxidized metallic lead exists in the anodic film. A small percentage of sulphur exists through the whole

---

* To whom correspondence should be addressed.

0021-891X

Table 1. Characteristic lines of XRD pattern of the anodic film on Pb–6 at % As at 0.9 V in 4.5 M H_2SO_4 solution (25° C) for 5 h

Characteristic lines d/nm (relative intensity)	*Width/degree*	*Evaluation compound, JCPDS file [d/nm (relative intensity)]**
0.4267 (21)	0.42	$PbSO_4$, [0.426 (87)]
0.3817 (16)	0.48	$PbSO_4$, [0.3813 (57)]
0.338 (20)	0.42	$PbO \cdot PbSO_4$, [0.334 (100)]; $PbSO_4$, [0.333 (86)]
0.3220 (16)	0.42	$PbSO_4$, [0.3220 (71)]
0.3125 (19)	0.54	*t*-PbO, [0.3115 (100)]
0.3009 (20)	0.45	$PbSO_4$, [0.3001 (100)]; $PbO \cdot PbSO_4$, [0.296(80)]
0.2859 (100)	0.42	Pb, [0.2855 (100)]; $PbO \cdot PbSO_4$, [0.285 (50)]
0.2811 (17)	0.48	*t*-PbO, [0.2809 (62)]
0.2699 (11)	0.39	$PbSO_4$, [0.270 (47)]
0.2553 (8)	0.36	$3PbO \cdot PbSO_4$, [0.251 (70)]
0.2476 (44)	0.42	Pb, [0.247 (50)]
0.2084 (9)	0.39	$3PbO \cdot PbSO_4$, [0.210 (70)]
0.2068 (14)	0.45	$PbSO_4$, [0.2067 (76)]
0.203 (12)	0.57	$PbSO_4$, [0.2028 (48)]
0.175 (49)	0.51	Pb, [0.175 (31)]; $3PbO \cdot PbSO_4$, [0.170 (60)]
0.1599 (6)	0.34	$3PbO \cdot PbSO_4$, [0.158 (100)]

* JCPDS cards: 5–0577 ($PbSO_4$), 5–0561 (*t*-PbO), 33–1486 ($PbO \cdot PbSO_4$), 2–1376 ($3PbO \cdot PbSO_4$) and 4–0686 (Pb).

anodic film due to the presence of basic lead sulphate. During the first 6 min of the sputtering period, the atomic percentage of lead declines gradually to 45%. At the same time, that of arsenic increases gradually to 13%, and that of oxygen also increases a little. It can be asserted that As(III) species penetrate into the corrosion layer during the anodic oxidation of the electrode.

3.3. *Potentiostatic growth of the anodic film*

Figure 2 shows the *i* against $t^{-1/2}$ curve for a Pb–6 at % As electrode anodizing at 0.9 V, where *i* denotes the anodizing current density and *t* the anodizing time.

If the dissolution of the anodic film is negligible during the oxidation process, the anodizing current may be regarded as the growth current of the anodic film. It is observed from Fig. 2 that there is a linear relationship between *i* and $t^{-1/2}$ and that the extrapolated line approaches the origin. Therefore, the growth of the anodic film is controlled by a diffusion mechanism. The value of $(\mathrm{d}i/\mathrm{d}t^{-1/2})$ obtained for a Pb–6 at % As electrode is 2.7 mA cm^{-2} s$^{1/2}$.

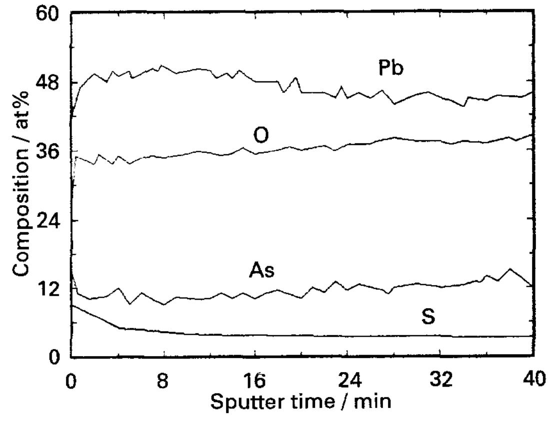

Fig. 1. Auger depth profile for the anodic film on Pb–6 at % As electrode formed at 0.9 V in 4.5 M H_2SO_4 for 2 h.

3.4. *Cyclic voltammetry*

Cyclic voltammograms for Pb and Pb–6 at % As electrodes were traced at a sweep rate of 2 mV s^{-1}. Typical cyclic voltammograms were obtained (Fig. 3). The positive potential scan was begun at the steady potentials of Pb and Pb–6 at % As electrodes, −0.962 V, and −0.958 V, respectively. During the positive scan, anodic peaks A1 appear at −0.915 V for both Pb and Pb–6 at % As electrodes, corresponding to the formation of $PbSO_4$. When the potential reaches −0.15 V, another anodic peak A2 appears for a Pb–6 at % As electrode. The peak potential is −0.072 V. There is no such characteristic peak for a lead electrode. It is reasonable to suggest that this peak is related to the anodization of arsenic.

During the negative potenital scan for lead electrode, a reduction peak C1 appears at −0.816 V, which represents the overlapping reduction peak of *t*-PbO and $PbO \cdot PbSO_4$ [5]. For the Pb–6 at % As

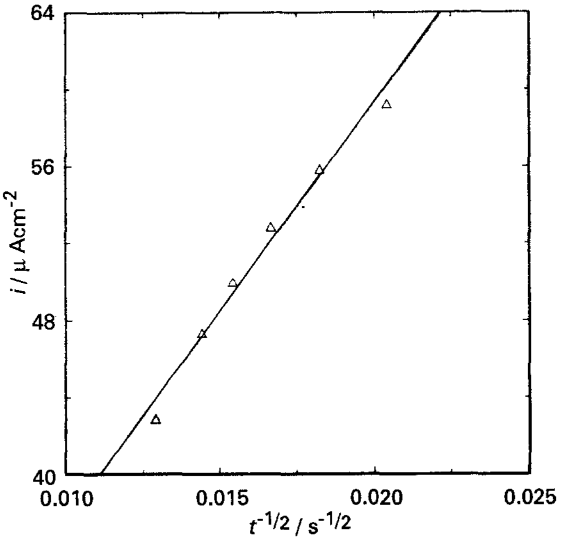

Fig. 2. *i* against $t^{-1/2}$ curve for Pb–6 at % As electrode at 0.9 V in 4.5 M H_2SO_4.

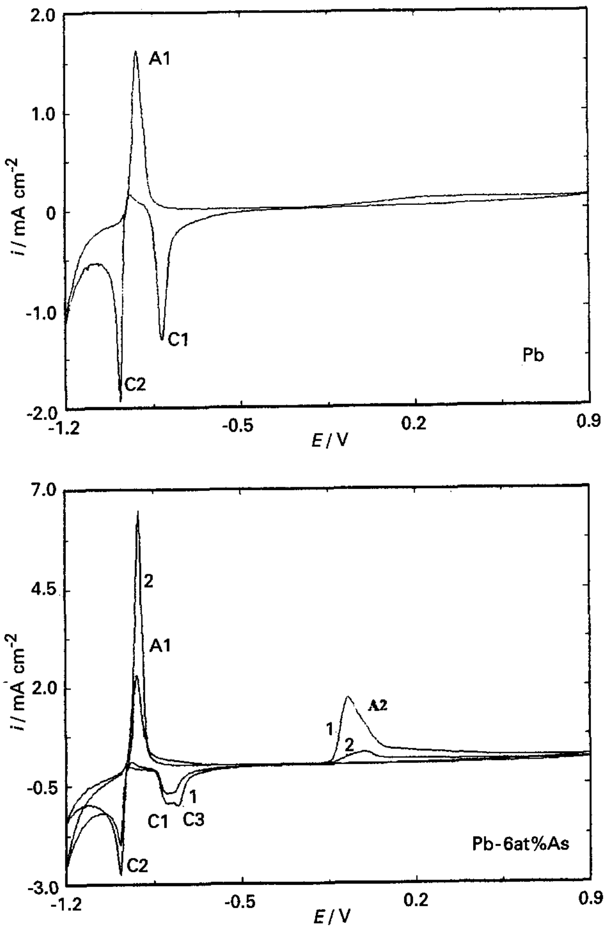

Fig. 3. Cyclic voltammograms for Pb (first cycle) and Pb–6 at % As (first two cycles) electrodes in 4.5 M H_2SO_4 (scan rate 2 mV s^{-1}). (1) First cycle and (2) second cycle.

electrode, it is obvious that reduction peaks C3 (−0.756 V) and C1 (−0.792 V) overlap during the negative potential scan. At the second cycle, the peak potential of C1 is the same as that of the first cycle, while the peak potential of C3 shifts towards the negative, closer than C1, and the peak current is considerably reduced. This coincides with the decrease of the peak A2. This indicates the peak C1 represents the reduction of lead oxide and C3 may be the reduction peak of the As(III) oxide formed at anodic peak A2. The positive shift of the peak potential of C1 may be due to the presence of 3PbO • $PbSO_4$ in the anodic film by comparison with the corresponding peak for a lead electrode. According to the above results, in addition to those of Auger depth profile (Fig. 1), it is likely that some arsenic compounds exist in the anodic film, probably As_2O_3 and AsO_2^-. The As_2O_3 formed during anodization is amorphous, since there are no diffraction lines of As_2O_3 in Table 1.

The reduction peak C2 corresponds to the reduction of $PbSO_4$ which is formed at anodic peaks A1 for both Pb and Pb–6 at % As electrodes.

3.5. *Equivalent circuit of the anodic film*

The impedance measured can be expressed as a parallel combination of a resistance (R_p) and a capacitance (C_p), i.e.

$$R_p^{-1} = Y' \quad (1)$$

$$j\omega C_p = Y'' \quad (2)$$

where Y' and Y'' are the in-phase component and out-of-phase component of the admittance, respectively. Equation 2 can be established, since there is no evidence of an inductance element in the experimental results, as is illustrated by the Bode plot shown in Fig. 4, which was measured at −0.2 V.

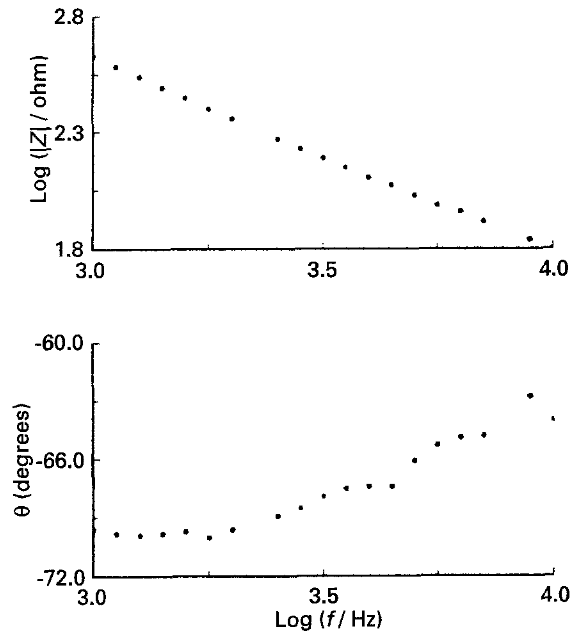

Fig. 4. Bode plots measured at −0.2 V for the film formed on Pb–6 at % As electrode at 0.9 V in 4.5 M H_2SO_4 for 2 h.

Figure 5(a) shows the equivalent circuit generally used to represent semiconductor electrodes [6]. It is adopted here for the analysis of the a.c. impedance data of the anodic film.

The resistances of the bulk film, the solution, and the contact between the electrode substrate and the film (R_o) may be neglected [7]. Generally, the capacitance of the Helmholtz layer (C_H) is about 20 μF cm^{-2}. Compared with C_p measured in the present work, C_H may be omitted in Fig. 5(a). Therefore the equivalent circuit Fig. 5(b) is used for the present work.

When the anodizing time is much longer, about 40 min, the impedance of the $PbSO_4$ layer may be neglected, compared with that of the anodic film formed on a Pb–6 at % As electrode.

In Fig. 5, C_{ss} and R_{ss} represent the capacitance and the resistance of the surface state and C_{sc} and R_{sc} the capacitance and resistance of the space charge region, respectively. These parameters may be calculated through the following equations:

$$R_p^{-1} = R_{sc}^{-1} + C_{ss}^2 R_{ss} \omega^2 [1 + (C_{ss} R_{ss} \omega)^2]^{-1} \quad (3)$$

$$C_p = C_{sc} + C_{ss} [1 + (C_{ss} R_{ss} \omega)^2]^{-1} \quad (4)$$

where ω denotes the angular frequency.

At low frequency, when $(C_{ss} R_{ss} \omega) \ll 1$, Equation 3

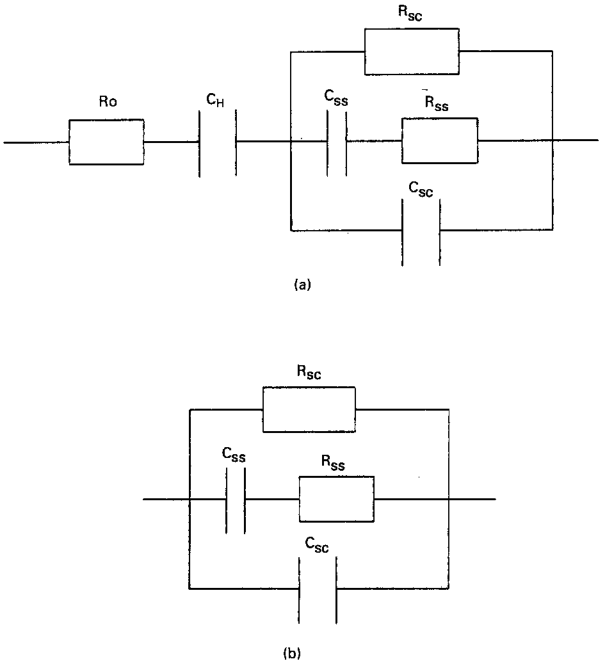

Fig. 5. Equivalent circuit for analysis of the impedance data for the anodic films.

can be simplified to:

$$R_p^{-1} = R_{sc}^{-1} + C_{ss}^2 R_{ss}\omega^2 \qquad (5)$$

Thus, R_{sc} can be obtained from the R_p^{-1} against ω^2 relation. In the present work, R_{sc} calculated according to the above method is much greater than R_p, thus, Equation 3 may be simplified to

$$R_p = R_{ss} + C_{ss}^{-2} R_{ss}^{-1} \omega^{-2} \qquad (6)$$

As R_{ss} and C_{ss} vary with frequency, they may be obtained from the relationship between R_p and ω^{-2} over a narrow range of frequencies. Thereafter, C_{sc} can be obtained according to Equation 4.

The parameters of the equivalent circuit of the anodic film obtained at 0.9 V for 2 h on Pb–6 at % As are shown in Table 2. The plot of R_p against ω^{-2} should be a straight line, as required by Equation 6. This is illustrated by the correlation coefficients listed in Table 2. It can be concluded that the equivalent circuit shown in Fig. 5(b) is valid for the present work.

3.6. *Relationship between C_p and t*

Figure 6 presents the dependence of the capacitance C_p at 2500 Hz on the reciprocal of the square root of anodization time for Pb–6 at % As at 0.9 V. If the space charge region in the film is a depletion layer, the thickness of the film is less than the Debye length, and the film is planar, then C_{sc} can be written as

$$C_{sc} = \epsilon\epsilon_o / L \qquad (7)$$

where ϵ_o denotes the permittivity of vacuum, ϵ the dielectric constant, and L the thickness of the space charge region. When the film is thin, the thickness of the space charge region can be represented by the film thickness.

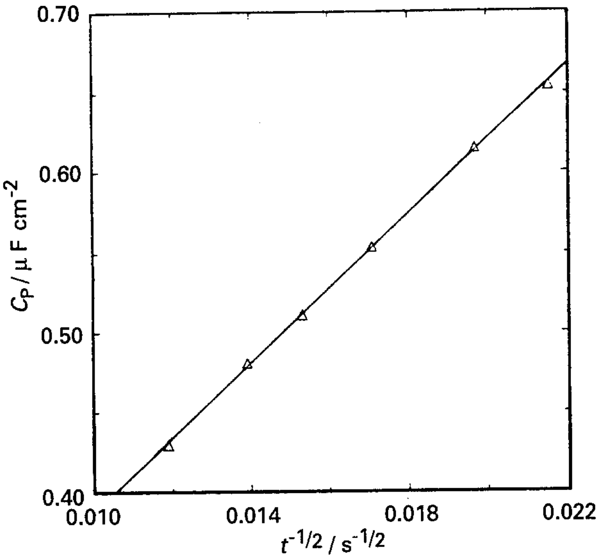

Fig. 6. C_p against $t^{-1/2}$ curve for Pb–6 at % As electrode at 0.9 V in 4.5 M H_2SO_4 at 2500 Hz.

With increase in anodizing time, the real space charge region increases, and the capacitance decreases. It may be assumed that the film is dense and obeys the equation

$$L = \frac{QV_m}{ZF} \qquad (8)$$

where V_m denotes the molar volume of $PbO \cdot PbSO_4$, Z the number of faradays for reduction of one mole of $PbO \cdot PbSO_4$ to lead and F is the Faraday constant. From Equations 7 and 8

$$C_{sc} = \epsilon\epsilon_o \frac{ZF}{QV_m} \qquad (9)$$

Thus

$$\left(\frac{dC_{sc}}{dt^{-1/2}}\right) = \epsilon\epsilon_o \frac{ZF}{V_m}\left(\frac{dQ}{dt^{1/2}}\right)^{-1} \qquad (10)$$

If C_{ss} and R_{ss} are both independent of time, then from Equations 4 and 10, the following relation is obtained:

$$\left(\frac{dC_p}{dt^{-1/2}}\right) = \epsilon\epsilon_o \frac{ZF}{V_m}\left(\frac{dQ}{dt^{1/2}}\right)^{-1} \qquad (11)$$

The linear relation between C_p and $t^{-1/2}$ for Pb–6 at % As at 0.9 V shown in Fig. 6 is good, and the extrapolated line approaches the origin. The dielectric constant of the anodic film can be calculated from the slopes in Figs 2 and 6. The value of $dQ/dt^{-1/2}$ in Equation 11 can be obtained from Fig. 2, according to $dQ = i dt$. The dielectric constant of the anodic film of Pb–6 at % As at 0.9 V thus can be calculated to be 2.8×10^2 at 2500 Hz.

3.7. *Mott–Schottky plot*

The Mott–Schottky equation for an n-type semi-

Table 2. Parameters in equivalent circuit at 2500 Hz for anodic film on Pb–6 at % As in 4.5 M H_2SO_4 at 0.9 V for 2 h

E* /V	f /kHz	R_p /kΩ cm^2	C_p /μF cm^{-2}	R_{ss} /kΩ cm^2	C_{ss} /μF cm^{-2}	C_{sc} /μF cm^{-2}	R†
0.90	1.8	1.365	0.1842	0.7203	0.1300	0.1431	0.998
	2.0	1.258					
	2.5	1.056					
	2.8	0.9700					
	3.2	0.9100					
0.40	1.8	1.306	0.1876	0.6961	0.1359	0.1452	0.997
	2.0	1.199					
	2.5	1.027					
	2.8	0.9363					
	3.2	0.8831					
0.0	1.8	1.163	0.2069	0.6107	0.1527	0.1584	0.996
	2.0	1.064					
	2.5	0.9020					
	2.8	0.8455					
	3.2	0.7701					
−0.10	1.8	1.042	0.2331	0.5273	0.1699	0.1761	0.994
	2.0	0.9493					
	2.5	0.8133					
	2.8	0.7420					
	3.2	0.6713					
−0.20	1.8	0.7501	0.3105	0.2767	0.2448	0.1957	0.998
	2.0	0.6670					
	2.5	0.5284					
	2.8	0.4707					
	3.2	0.4187					
−0.30	1.8	0.3516	0.4262	0.1599	0.5068	0.2329	0.997
	2.0	0.3160					
	2.5	0.2638					
	2.8	0.2377					
	3.2	0.2166					

* E is the potential at which the impedance of the anodic film is measured.
† Correlation coefficient between R_p and ω^{-2}.

conductor is given by [8]:

$$C_{sc}^{-2} = 2\frac{(E - E_{fb} - kT/e)}{\epsilon\epsilon_0 e N_D} \qquad (12)$$

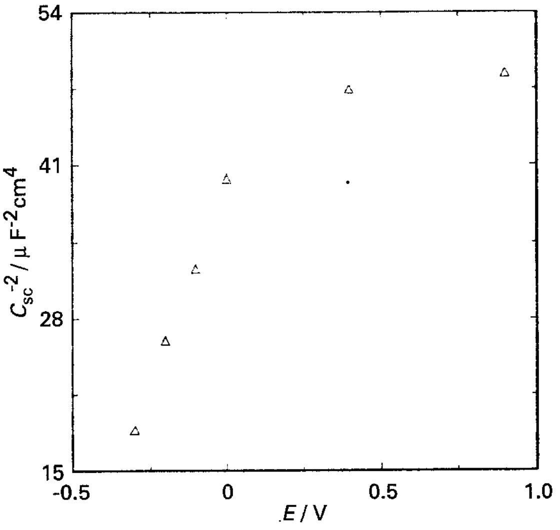

Fig. 7. Mott–Schottky plot of the anodic film formed on Pb–6 at % As at 0.9 V in 4.5 M H_2SO_4 for 2 h at 2500 Hz.

where E denotes the potential of the electrode, E_{fb} the flat-band potential, k the Boltzmann constant, T the absolute temperature, e the elementary charge and N_D the donor density.

The values of C_{sc} used for the Mott–Schottky plot are listed in Table 2. Figure 7 gives the C_{sc}^{-2} against E curve of the anodic film measured at 2500 Hz for Pb–6 at % As. The result shows the film is an n-type semiconductor. The value of E_{fb} for the film on Pb–6 at % As is −0.56 V. The donor density is 7.2×10^{15} cm^{-3}. Compared with the N_D of the anodic film on lead, 8.2×10^{15} cm^{-3} [7], the existence of arsenic in the lead alloy causes the donor density of the anodic film to decrease. This may be due to the fact that the film contains an insulator of As_2O_3.

The thickness of the space charge region increases with increasing potential. The film studied in the present work is so thin that the thickness of the film is less than that of the space charge region at high potentials, at which C_{sc} is nearly constant. Therefore, the curve in Fig. 7 cannot fit the Mott–Schottky equation at high potentials.

Acknowledgement

This work was financially supported by the National Natural Science Foundation of China.

References

[1] D. Pavlov, A. Dakhouche and T. Rogachev, *J. Power Sources* **30** (1990) 117.

[2] A. A. Abdul Azim and A. A. Ismail, *J. Appl. Electrochem.* **7** (1977) 119.

[3] I. H. Yeo and D. C. Johnson, *J. Electrochem. Soc.* **134** (1987) 1973.

[4] W.-F. Zhou and X.-L. Chen, *Acta Chimica Sinica* **43** (1985) 333.

[5] J. Han, C. Pu and W.-F. Zhou, *J. Electroanal. Chem.* in press.

[6] S. R. Morrison, *in* 'Electrochemistry at Semiconductor and Oxidized Metal Electrodes', Plenum, Press, New York (1980) p. 124.

[7] C. Pu, Ph.D. thesis, Fudan University, Shanghai, China (1991).

[8] R. Memming, *in* 'Comprehensive Treatise of Electrochemistry', Vol. 7 (edited by B. E. Conway, J. O'M. Bockris, E. Yeager, S. U. M. Khan and R. E. White), Plenum Press, New York (1983) p. 553.